Supporting Information

Hydrogen-bonded macrocycle-mediated dimerization for orthogonal supramolecular polymerization

Wentao Yu, Zhiyao Yang, Chengkan Yu, Xiaowei Li* and Lihua Yuan*

College of Chemistry, Sichuan University, Chengdu 610064, China;
ywt1255751521@163.com (W.Y.); yangzhiyaoha-ha@sina.com (Z.Y.);
yuchengkan@stu.scu.edu.cn (C. Y.)

** Correspondence: lhyuan@scu.edu.cn (L.Y.); lixw@scu.edu.cn (X.L.)*

Table of Contents

Synthesis and characterization

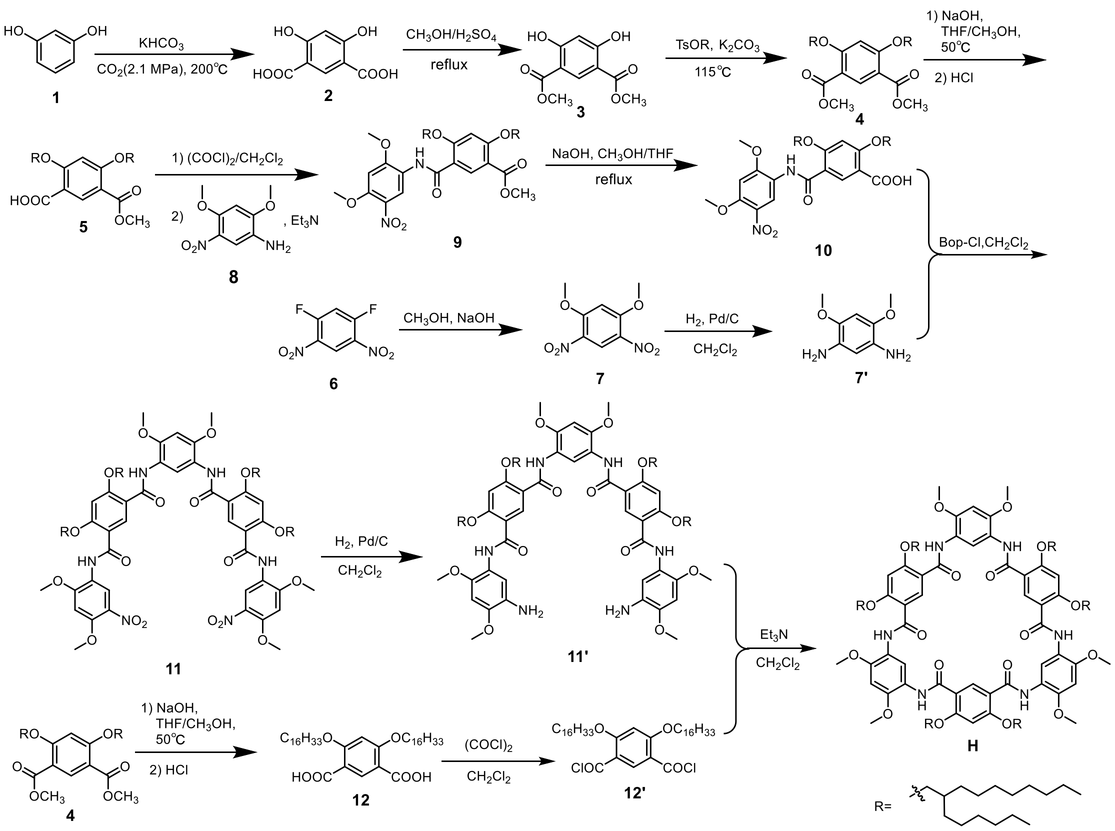

Scheme S1 Synthetic route of **H**.

H was prepared according to literature procedures. [1]

H: white solid powder (yield: 64 %). ^{1}H NMR (400 MHz, $CDCl_3$, 298 K): δ 9.98 (s, 2H), 9.75 (s, 4H), 9.24 (d, *J* = 2.6 Hz, 4H), 7.99 (dd, *J* = 8.7, 2.7 Hz, 4H), 7.09 (d, *J* = 8.8 Hz, 4H), 6.53 (s, 2H), 4.15 (d, *J* = 6.3 Hz, 8H), 3.91 (s, 12H), 2.12 (p, *J* = 6.2 Hz, 4H), 1.63–1.15 (m, 108H), 0.85 (m, 24H).

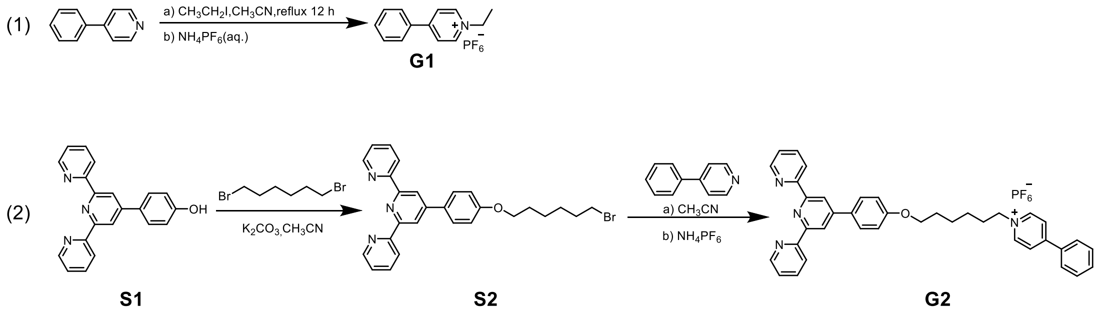

Scheme S2 Synthetic routes of guests **G1** and **G2**.

Guest **G1** [2]

Synthesis of **G1**: A mixture of 4-phenylpyridine (2 g, 4.80 mmol), ethyl iodide (2 mL, 6.00 mmol) in 2 mL of acetonitrile was stirred at 90 °C for 24 h. After the reaction solution was cooled down, the solvent was concentrated, and washed with ethyl ether to obtain a white solid powder with a yield of 90%. Ion exchange: dissolve the white solid in 5 mL of methanol, gradually add saturated aqueous solution of NH_4PF_6, precipitate white solid powder, filter and dry to obtain the compound **G1** whose counter ion is hexafluorophosphate. ^{1}H NMR (400 MHz, Methanol-d4) δ 8.99 (d, *J* = 7.1 Hz, 2H), 8.41 (d, *J* = 6.9 Hz, 2H), 8.01 (dd, *J* = 6.7, 2.9 Hz, 2H), 7.68 – 7.61 (m, 3H), 4.69 (q, *J* = 7.3 Hz, 2H), 1.69 (t, *J* = 7.3 Hz, 3H).

S2 [3]

Synthesis of **S2**: A mixture of **S1** (500 mg, 1.54 mmol), 1,6-dibromohexane (1.12 g, 4.61 mmol), potassium carbonate (510 mg, 3.69 mmol) in 180 mL of acetonitrile was stirred at 100 °C for 24 h. The reaction solution was cooled down, and the solvent was concentrated. After the reaction solution was cooled, the solvent was concentrated, the precipitate was filtered and washed with acetonitrile for three times (3×25 mL), a white solid powder was obtained with 80% yield. ^{1}H NMR (400 MHz, Acetone-*d₆*) δ 8.80 (s, 2H), 8.75 (d, *J* = 1.5 Hz, 2H), 8.75 – 8.73 (m, 2H), 8.00 (td, *J* = 7.7, 1.8 Hz, 2H), 7.93 – 7.90 (m, 2H), 7.50 – 7.46 (m, 2H), 7.19 – 7.16 (m, 2H), 4.13 (t, *J* = 6.4 Hz, 2H), 3.54 (t, *J* = 6.8 Hz, 2H), 1.94 (d, *J* = 7.0 Hz, 2H), 1.86 (d, *J* = 6.7 Hz, 2H), 1.57 (p, *J* = 3.5 Hz, 4H).

Guest **G2** [4,5]

Synthesis of **G2**: A mixture of **S2** (300 mg, 614 μmol), 4-phenylpyridine (95 mg, 614 μmol) in 10 mL of acetonitrile was stirred at 110 °C for 24 h. A white solid was obtained by filtration under reduced pressure, and the white solid powder was obtained by washing with ether in a yield of 85%.

Ion exchange: The solid was dissolved in CH_3CN/H_2O (1:1, *v:v*) and saturated aqueous NH_4PF_6 was added. The organic solvent was then evaporated under reduced pressure. The precipitate was collected and washed with H_2O, filter and dry to get the compound **G2** with hexafluorophosphate as the counter ion. ^{1}H NMR (400 MHz, $CDCl_3$) δ 8.73 (d, *J* = 4.3 Hz, 2H), 8.69 (s, 3H), 8.65 (d, *J* = 7.0 Hz, 3H), 8.20 (s, 2H), 7.98 (d, *J* = 6.8 Hz, 2H), 7.86 (d, *J* = 7.0 Hz, 4H), 7.62 (d, *J* = 6.9 Hz, 3H), 7.47 – 7.41 (m, 2H), 7.05 (s, 2H), 4.52 (d, *J* = 7.4 Hz, 2H), 4.06 (d, *J* = 6.3 Hz, 2H), 2.06 (d, *J* = 7.6 Hz, 2H), 1.85 (t, *J* = 7.2 Hz, 2H), 1.59 (d, *J* = 7.8 Hz, 2H), 1.48 (d, *J* = 7.5 Hz, 2H).

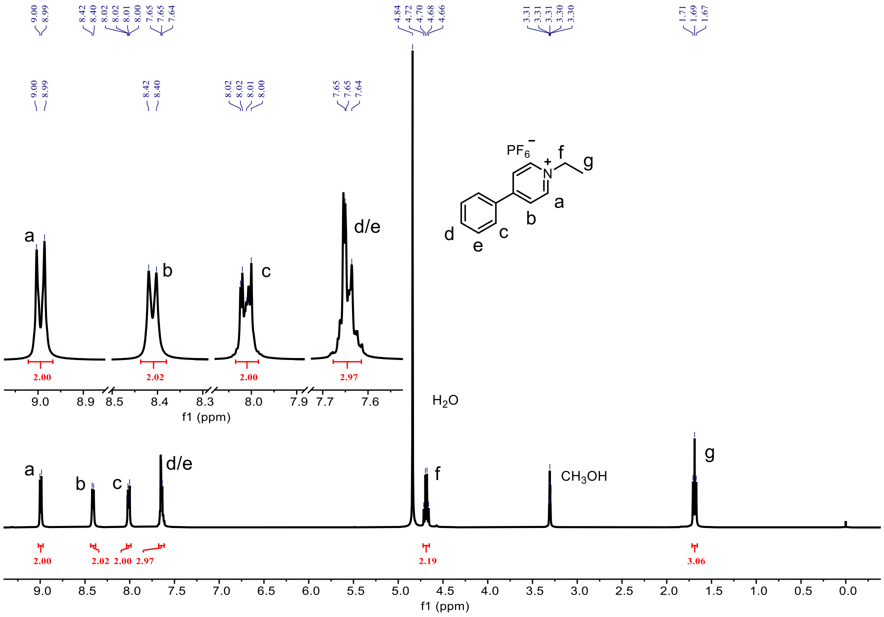

Figure S1 ^{1}H NMR spectrum (400 MHz, CD$_3$OD, 298 K) of **G1**.

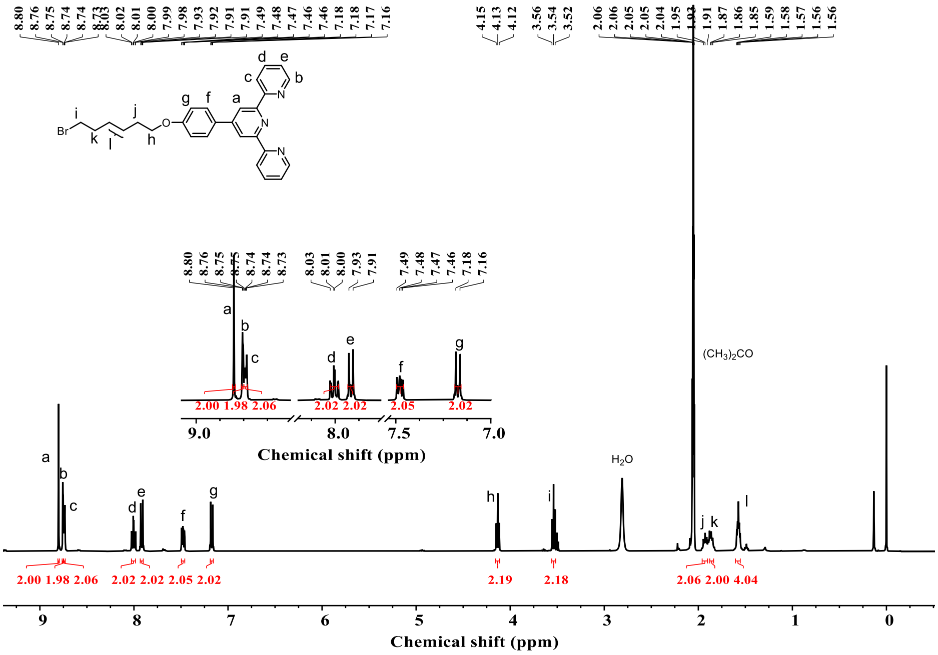

Figure S2 ^{1}H NMR spectrum (400 MHz, CD$_3$COCD$_3$, 298 K) of **S2**.

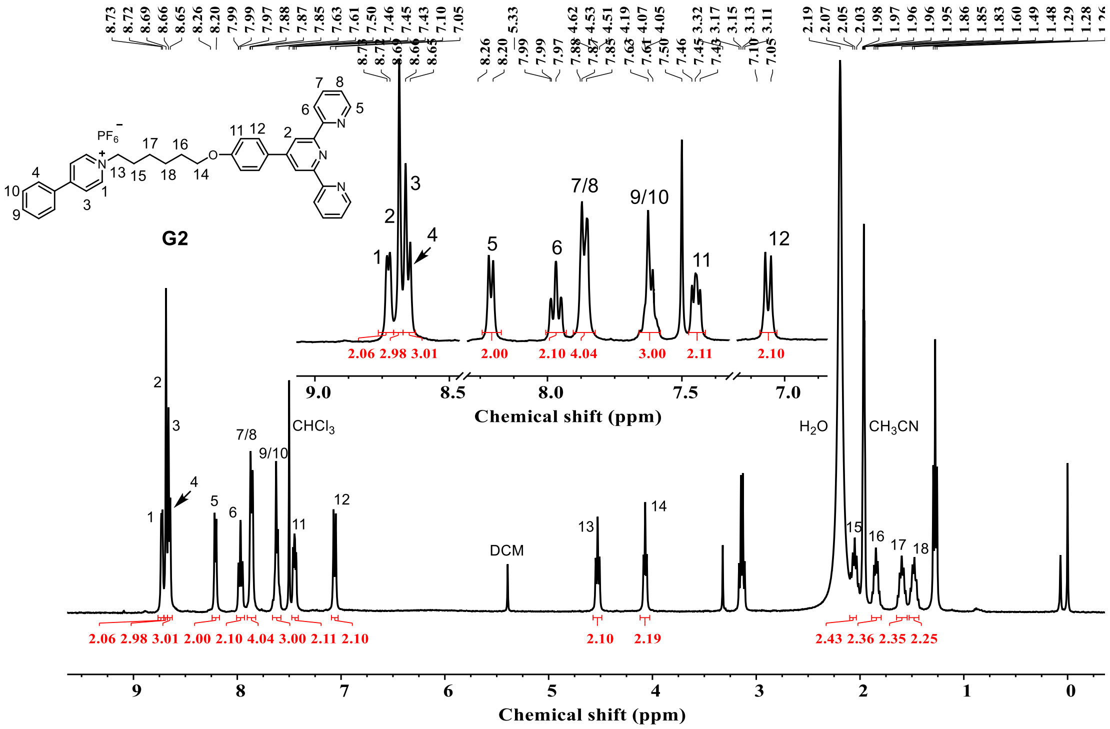

Figure S3 ^{1}H NMR spectrum (400 MHz, $CDCl_3$, 298 K) of **G2**.

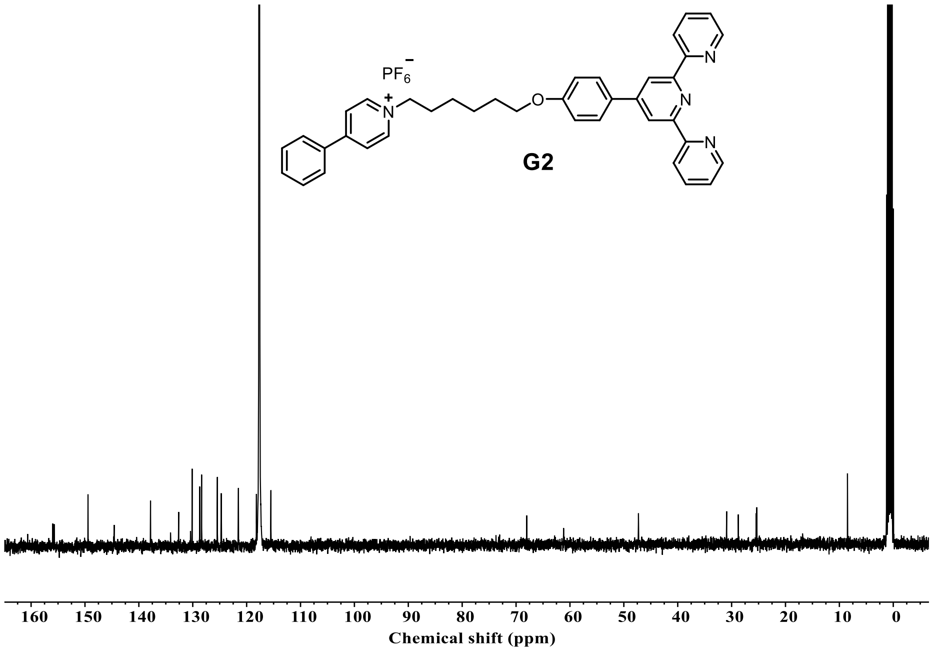

Figure S4 ^{13}C NMR spectrum of **G2** (100 MHz, CD_3CN, 298 K).

Stacked ^{1}H NMR spectra for **H** and **G1** interactions

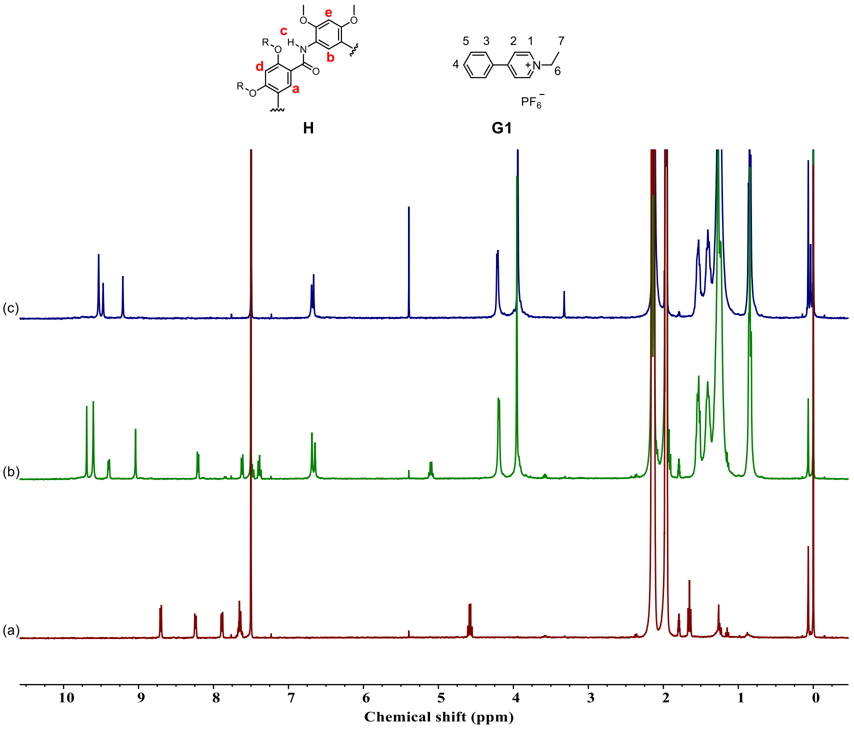

Figure S5 Stacked ^{1}H NMR spectra of (a) **G1**; (b) **H**:**G1**=1:1; (c) **H**.(400 MHz, $CDCl_3/CD_3CN$=1:1, *v:v*, 298 K). [**H**]= [**G1**] =1.0 mM.

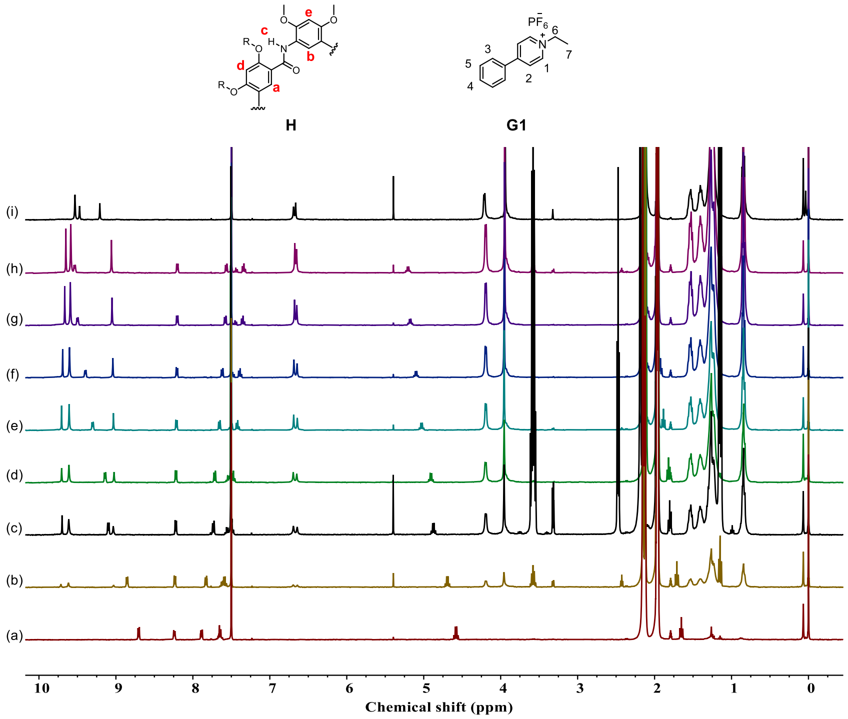

Figure S6 Stacked ^{1}H NMR spectra ($CDCl_3/CD_3CN$, 1:1, *v/v*, 400 MHz, 298 K) of **G1** upon addition of different equiv of **H** ([**G1**] = 1.0×10^{-3} M, [**H**]/[**G1**] = 0 – 1.4 eq). (a) 0.0 eq, (b) 0.2 eq, (c) 0.4 eq, (d) 0.6 eq, (e) 0.8 eq, (f) 1.0 eq, (g) 1.2 eq, (h) 1.4 eq, and (i) only **H**.

Stacked ^{1}H NMR spectra for **H** and **G2** interactions

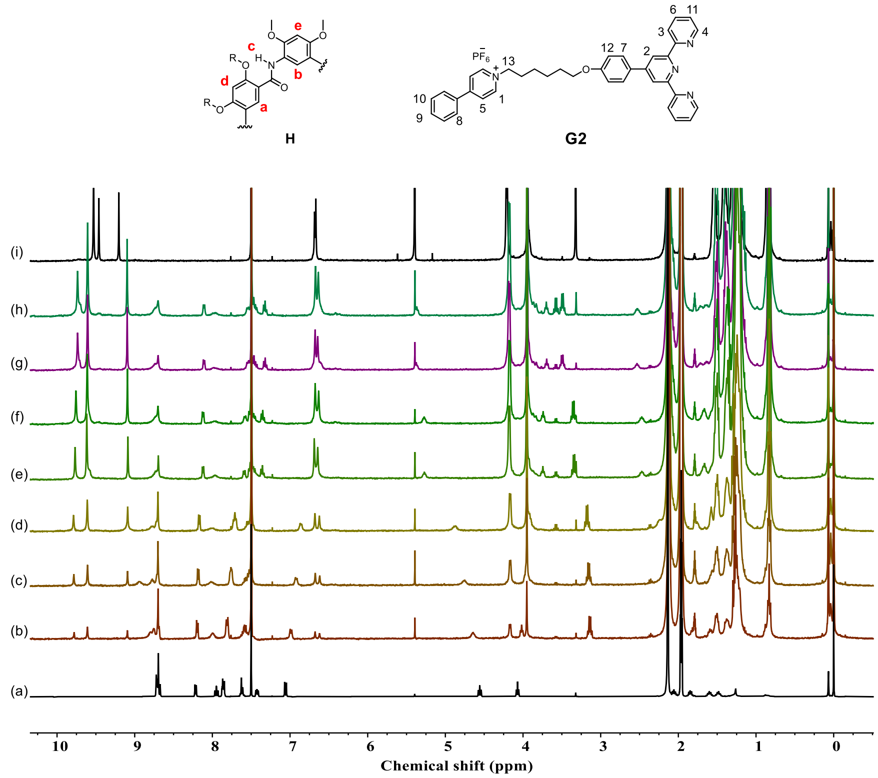

Figure S7 Stacked ^{1}H NMR spectra ($CDCl_3/CD_3CN$, 1:1, v/v, 400 MHz, 298 K) of **G2** upon addition of different equiv of **H** ([**G2**] = 1.0 × 10^{-3} M, [**H**]/[**G2**] = 0 – 1.4 eq). (a) 0.0 eq, (b) 0.2 eq, (c) 0.4 eq, (d) 0.6 eq, (e) 0.8 eq, (f) 1.0 eq, (g) 1.2 eq, (h) 1.4 eq, and (i) only **H**

^{1}H NMR spectra for **G2** and **Zn(ClO$_4$)$_2$** interactions

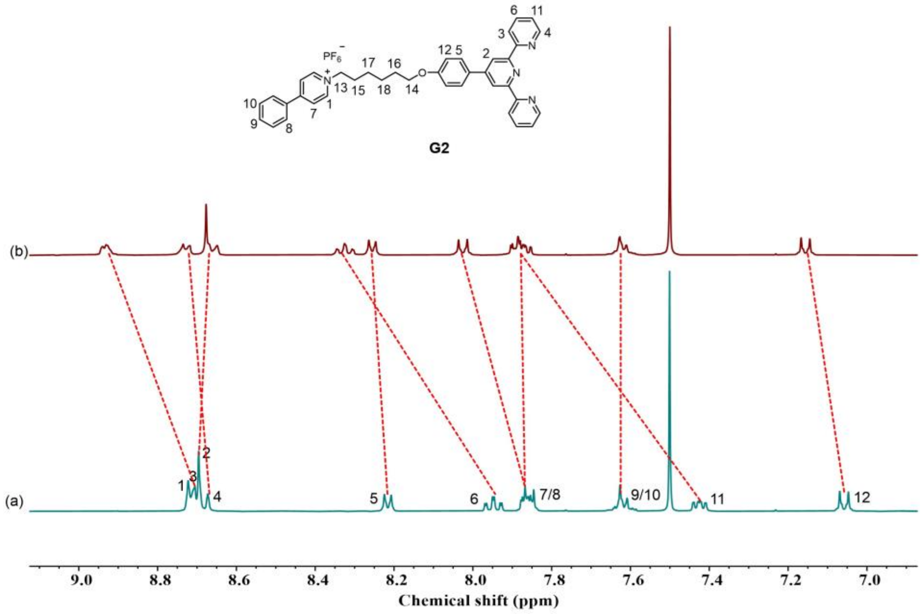

Figure S8 Stacked ^{1}H NMR spectra of (a) **G2**; (b) **G2**:Zn^{2+}=1:1. (400 MHz, $CHCl_3/CH_3CN$=1:1, *v:v*, 298 K). [Zn^{2+}] = [**G2**] =1.0 mM.

Job plot for the determination of stoichiometry of host-guest complexes

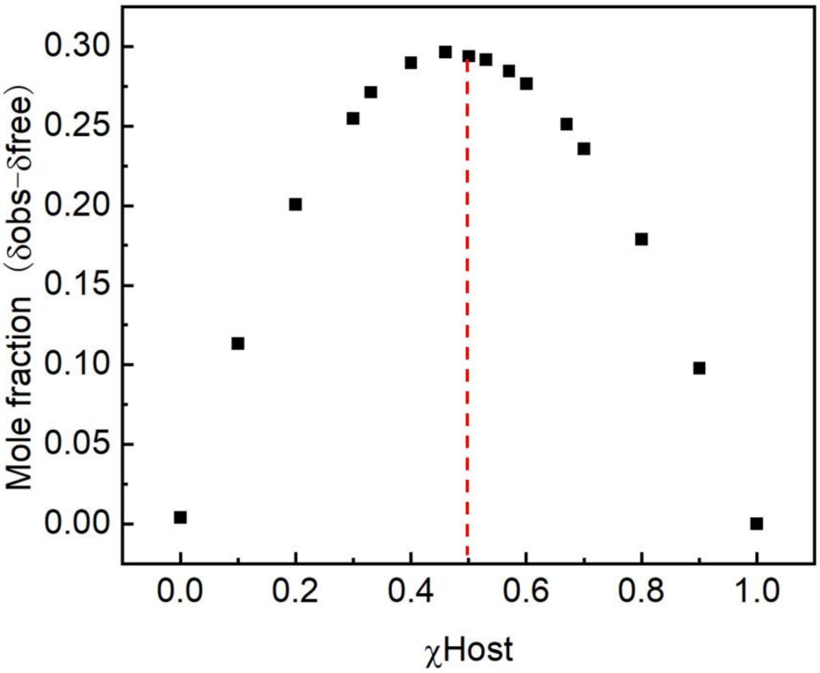

Figure S9 Job plot showing a peak maximum was reached around 0.5 corresponding to the formation of a n:n host-guest complex between **H** and **G1**. [**H**] + [**G1**] = 50 μM.

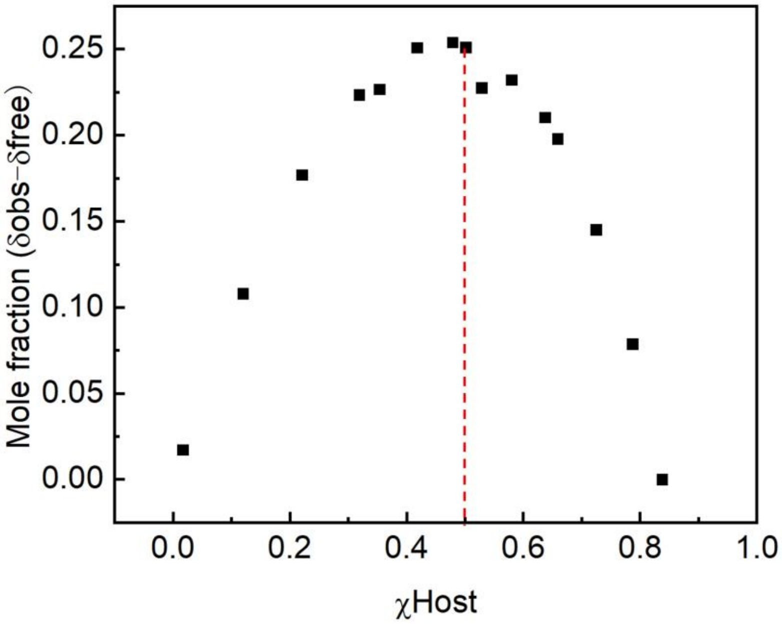

Figure S10 Job plot showing a peak maximum was reached around 0.5 corresponding to the formation of a n:n host-guest complex between **H** and **G2**. [**H**] + [**G2**] = 50 μM.

UV-vis titration experiments of macrocycle **H** and guest **G2**

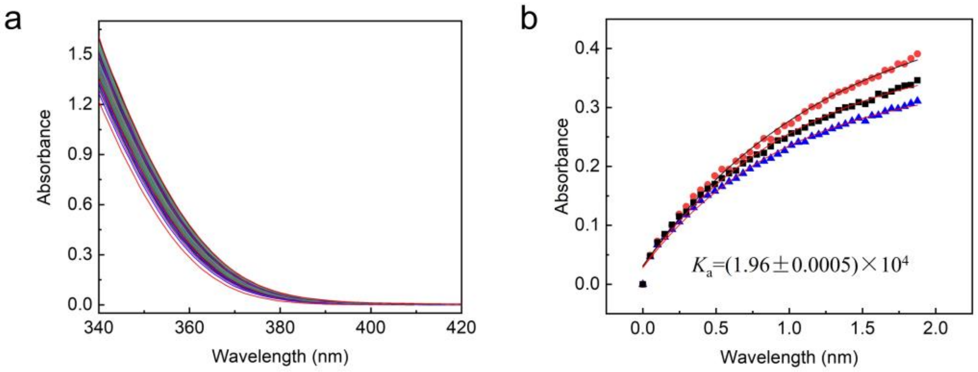

Figure S11 (a) Stacked UV-vis spectra of **H** (50 μM) titrated with **G2** from 0 equiv. to 2.0 equiv. in $CHCl_3/CH_3CN$ (1:1, *v/v*, 298 K). (b) Curve fitting of the binding constant of **G2** ⊂ **H** in $CHCl_3/CH_3CN$ (1:1, *v/v*, 298 K). The reported binding constant is the average value based on fitting of the absorbance at 333 nm, 357 nm, and 365 nm.

HRMS spectra of host-guest complexes **H** + **G2**.

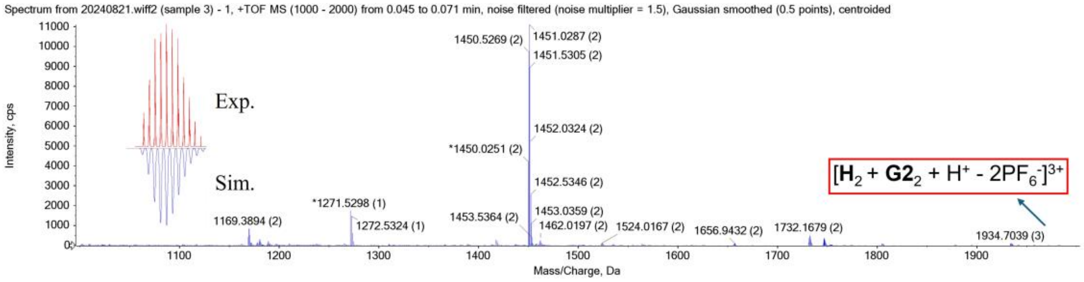

Figure S12 HR-MS of **H** ⊃ **G2** complex in $CHCl_3/CH_3CN$ 1:1, *v/v*). The calculated (blue) and experimental (red) isotopic distribution for $[\mathbf{H_2} + \mathbf{G2}_2 + H^+ - 2PF_6^-]^{2+}$, m/z, 1933.7006, found 1934.7039.

X-ray crystal structure of **G1** ⊂ **H**

Crystallographic data (excluding structure factors) for **G1** ⊂ **H** reported in this communication have been deposited with the Cambridge Crystallographic Data Centre as supplementary publication no. CCDC–2384953. Data collection and structure refinement details can be found in the CIF files or obtained free of charge via www.ccdc.cam.ac.uk/data_request/cif.

Table S1 Crystallographic data and structure refinement for **G1** ⊂ **H**

Identification code	**G1** ⊂ **H**
Empirical formula	$C_{96}H_{121}F_6N_8O_{18}P$
Formula weight	1819.98
Temperature/K	123(2)
Crystal system	monoclinic
Space group	P21/c
a/Å	24.434(4)
b/Å	20.026(3)
c/Å	23.779(4)
α/°	90.00
β/°	118.706(2)
γ/°	90.00
Volume/Å3	10205(3)
Z	4
ρcalcg/cm3	1.185
μ/mm-1	0.103
F(000)	3864.0
Crystal size/mm3	0.28 × 0.21 × 0.18
Radiation	MoKα (λ = 0.71073)
2Θ range for data collection/°	2.82 to 50.2
Index ranges	-29 ≤ h ≤ 29, -20 ≤ k ≤ 23, -28 ≤ l ≤ 21
Reflections collected	48435
Independent reflections	17763 [R_{int} = 0.0643, R_{sigma} = 0.0840]
Data/restraints/parameters	17763/2166/1263
Goodness-of-fit on F2	1.173
Final R indexes [I>=2σ (I)]	R_1 = 0.1072, wR_2 = 0.2846
Final R indexes [all data]	R_1 = 0.1709, wR_2 = 0.3153
Largest diff. peak/hole / e Å-3	0.92/-0.52

DLS data of **G2** + $Zn(ClO_4)_2$ and **H** + **G2** + $Zn(ClO_4)_2$

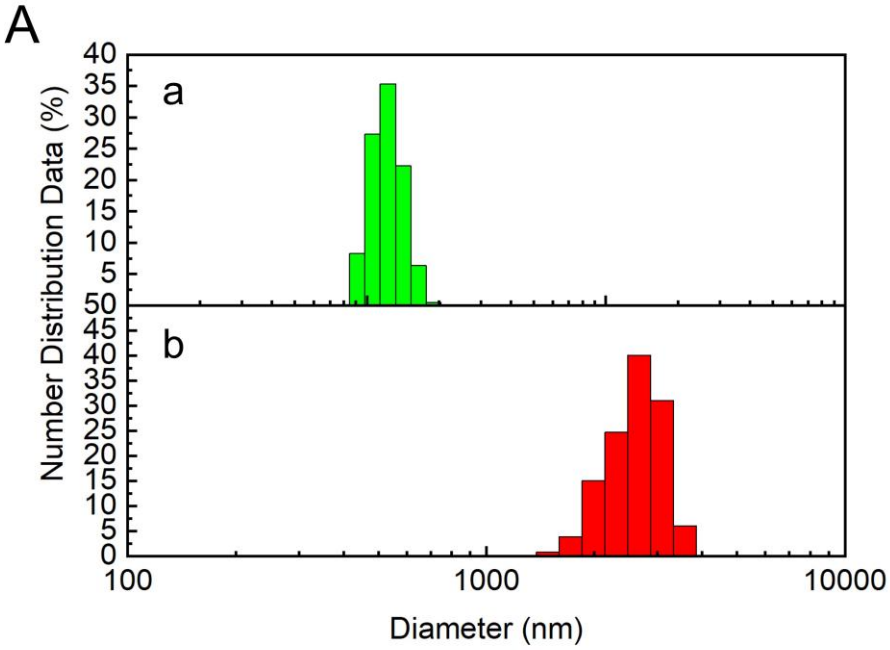

Figure S13 DLS of (a) **G2** + $Zn(ClO_4)_2$; (b) **H** + **G2** + $Zn(ClO_4)_2$. Solvent: $CHCl_3/CH_3CN$, 1:1, *v/v*, 298 K.

TEM of **H** + **G2** + $Zn(ClO_4)_2$ at variable concentration

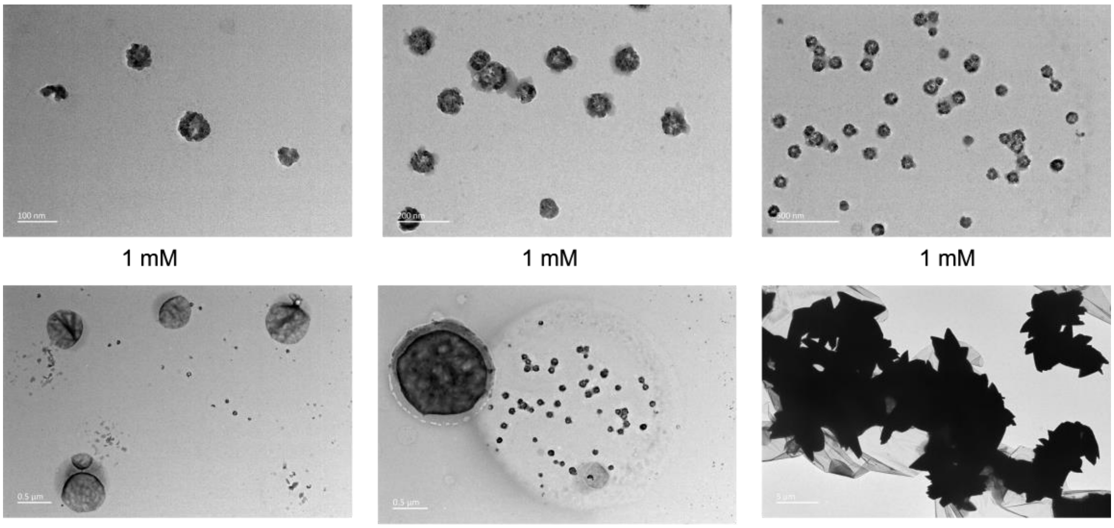

1 mM 1 mM 1 mM

3 mM 3 mM 5 mM

Figure S14 TEM images of **H**:**G2**:Zn^{2+}=1:1:1 at different concentrations ($CHCl_3/CH_3CN$ = 1:1, v/v, 298K).

Refrences

[1] Li, X.; Li, B.; Chen, L.; Hu, J.; Wen, C.; Zheng, Q.; Wu, L.; Zeng, H.; Gong, B.; Yuan, L. Liquid-Crystalline Mesogens Based on Cyclo[6]aramides: Distinctive Phase Transitions in Response to Macrocyclic Host-Guest Interactions. *Angew. Chem. Int. Ed.* **2015**, *54*, 11147–11152.

[2] Luo, L.; Tang, J.; Sun, R.; Li, W.; Zheng, X.; Yuan, M.; Li, R.; Chen, H.; Fu, H., Direct C–H Sulfonylimination of Pyridinium Salts. *Org. Lett.* **2022**, *24*, 2821-2825.

[3] T. Ogoshi, T. Aoki, R. and T.-a. Yamagishi. *J. Am. Chem. Soc.* **2012**, *134*, 20322−20325.

[4] G. Yu, J. Zhou, and X. Chi. *Macromol. Rapid Commun*., **2015**, *36*, 23−30.

[5] Wu, L.; Han, C.; Wu, X.; Wang, L.; Caochen, Y.; Jing, X. Reversible formation of supramolecular polymer networks via orthogonal pillar[10]arene-based host–guest interactions and metal ion coordinations. *DALTON. T*. **2015**, *44*, 20334-20337.

[6] Gaussian 09, Revision E.01, M. J. Frisch, G. W. Trucks, H. B. Schlegel, G. E. Scuseria, M. A. Robb, J. R. Cheeseman, G. Scalmani, V. Barone, B. Mennucci, G. A. Petersson, H. Nakatsuji, M. Caricato, X. Li, H. P. Hratchian, A. F. Izmaylov, J. Bloino, G. Zheng, J. L. Sonnenberg, M. Hada, M. Ehara, K. Toyota, R. Fukuda, J. Hasegawa, M. Ishida, T. Nakajima, Y. Honda, O. Kitao, H. Nakai, T. Vreven, J. A. Montgomery, Jr., J. E. Peralta, F. Ogliaro, M. Bearpark, J. J. Heyd, E. Brothers, K. N. Kudin, V. N. Staroverov, T. Keith, R. Kobayashi, J. Normand, K. Raghavachari, A. Rendell, J. C. Burant, S. S. Iyengar, J. Tomasi, M. Cossi, N. Rega, J. M. Millam, M. Klene, J. E. Knox, J. B. Cross, V. Bakken, C. Adamo, J. Jaramillo, R. Gomperts, R. E. Stratmann,O. Yazyev, A. J. Austin, R. Cammi, C. Pomelli, J. W. Ochterski, R. L. Martin, K. Morokuma, V. G. Zakrzewski, G. A. Voth, P. Salvador, J. J. annenberg, S. Dapprich, A. D. Daniels, O. Farkas, J. B. Foresman, J. V. Ortiz, J. Cioslowski, and D. J. Fox, Gaussian, Inc., Wallingford CT, 2013.